Available online at www.sciencedirect.com
SCIENCE DIRECT
Biochemical Pharmacology 69 (2005) 641–655
Biochemical Pharmacology
www.elsevier.com/locate/biochempharm

Multiple P2X and P2Y receptor subtypes in mouse J774, spleen and peritoneal macrophages

Robson Coutinho-Silva[a,e], David M. Ojcius[c], Darek C. Górecki[d], Pedro M. Persechini[e], Rodrigo C. Bisaggio[e], Anderson N. Mendes[e], Joanne Marks[b], Geoffrey Burnstock[a,*], Philip M. Dunn[a]

[a]*Autonomic Neuroscience Institute, Royal Free and University College Medical School, Rowland Hill Street, London NW3 2PF, UK*
[b]*Department of Physiology, Royal Free and University College Medical School, Rowland Hill Street, London NW3 2PF, UK*
[c]*Division of Natural Sciences, University of California, Merced, CA 95344, USA*
[d]*Institute of Biomedical and Biomolecular Sciences, School of Pharmacy and Biomedical Sciences, University of Portsmouth, Portsmouth, UK*
[e]*Instituto de Biofisica Carlos Chagas Filho, Universidade Federal do Rio de Janeiro, Rio de Janeiro, Brazil*

Received 23 June 2004; accepted 18 November 2004

Abstract

We investigated P2 receptor expression and function in macrophages from mouse, and in the J774 cell line, and revealed a larger spectrum of P2 receptor subtypes than previously recognised. The nucleotides adenosine triphosphate (ATP), adenosine diphosphate, uridine triphosphate and uridine diphosphate evoked an increase in intracellular calcium and the activation of a potassium current. The sensitivity of these responses to the antagonists suramin, PPADS, MRS 2179 and Cibacron blue suggest the presence of at least three functional P2Y receptor subtypes, most probably $P2Y_2$, $P2Y_4$ and $P2Y_6$. ATP also activated P2X receptors, giving rise to a rapidly activating cation conductance. This response was insensitive to the antagonists suramin and Cibacron blue, was potentiated by Zn^{2+} and inhibited by acidification suggesting involvement of $P2X_4$ receptors. In low divalent cation solution, responses to ATP became larger, and dibenzoyl-ATP became more potent than ATP, indicating the presence of $P2X_7$ receptors. Immunofluorescence, flow cytometry, Western blots and RT-PCR show that $P2X_4$ and $P2X_7$ receptors are the most prominent in both macrophage types, while the expression of the other P2X subunits is variable and sometimes weak or undetectable. These techniques also demonstrated the presence of mRNA for $P2Y_1$, $P2Y_2$, $P2Y_4$ and $P2Y_6$ receptors along with protein expression for the three subtypes we investigated, namely, $P2Y_1$, $P2Y_2$ and $P2Y_4$.

Keywords: Adenosine triphosphate; Purinergic receptors; Inflammation; Macrophages; Immunohistochemistry; Patch-clamp; Fura-2

1. Introduction

Adenosine 5′ triphosphate (ATP) is now recognised as an important extracellular signalling molecule and evokes a variety of physiological responses in many different tissues and cell types [1]. Most of the biological effects of extracellular ATP are mediated by P2 receptors, of which, there are two major classes: the nucleotide-gated ion-channel P2X receptors and G-protein-coupled P2Y receptors [2]. To date, seven mammalian P2X receptor subunits ($P2X_1$–$P2X_7$) have been identified, which assemble to form either homomeric or heteromeric receptors. Eight mammalian P2Y receptor subtypes ($P2Y_1$, $P2Y_2$, $P2Y_4$, $P2Y_6$, $P2Y_{11}$, $P2Y_{12}$ $P2Y_{13}$, and $P2Y_{14}$) and a structurally related but pharmacologically different homologue (at present called $P2Y_{15}$) have so far been cloned [3–7]. These receptors have different but overlapping pharmacological properties, and because many cell types express multiple P2 receptor subtypes, definitive identification of native receptors is often difficult.

Macrophages provide an important defence against pathogenic infection. Extracellular nucleotides have mul-

Abbreviations: BSS, balanced salt solution; NHS, normal horse serum; NGS, normal goat serum; MFI, mean fluorescence intensity

* Corresponding author. Tel.: +44 2078302948; fax: +44 2078302949.
E-mail address: g.burnstock@ucl.ac.uk (G. Burnstock).

0006-2952/$ – see front matter © 2004 Published by Elsevier Inc.
doi:10.1016/j.bcp.2004.11.012

tiple effects on these cells, including increasing pinocytic vesicle formation [8], superoxide generation [9], IL-1β release [10,11] and increased killing of infecting Chlamydia [12]. Early studies of the effects of nucleotides on mouse J774 macrophages showed that high concentrations of ATP caused a cation flux and permeablization due to the activation of the P2Z/$P2X_7$ receptor [13], while lower concentrations of ATP and UTP elevated intracellular calcium through the activation of a P2Y receptor, thought to be $P2Y_2$ [14]. However, a later study [15] could only detect mRNA for the $P2Y_6$ receptor in J774 macrophage cells. Studies on the effects of nucleotides on immune and inflammatory cells have concentrated on these two receptors [16]. However, there is increasing evidence that $P2X_7$ receptors are expressed in cell types outside the immune system [17–21], and that other P2 receptors may be expressed with $P2X_7$ and $P2Y_2$ on cells of the immune system, including B lymphocytes [22], thymocytes [23], macrophages and human dendritic cells [24,25].

Although the mRNA for various P2X and P2Y receptors has been identified in human blood-derived macrophages [24], the identity of the receptors responsible for functional responses has not been determined. More recently, a study of a rat alveolar macrophage cell line has indicated the involvement of $P2X_4$, $P2Y_1$ and $P2Y_2$ receptors [26]. However, the presence of different P2X and P2Y receptor subtypes in murine macrophages has not previously been explored. In this study, we investigated the expression of P2X and P2Y receptor subtype mRNA and protein in mouse spleen, and peritoneal macrophages and J774 cells using immunofluorescence, flow cytometry, and RT-PCR. We have followed this by looking for functional expression of these receptors using electrophysiology and measurement of intracellular Ca^{2+}. The significance of P2 receptor expression and correlations with macrophage physiology are discussed.

2. Materials and methods

2.1. Culture of J774 cells

Cultures of the J774 murine macrophage cells were grown in 25 ml tissue culture flasks at 37 °C in a 5% CO_2 humidified atmosphere. The culture medium comprised RPMI-1640 medium (Gibco BRL, Paisley Scotland) supplemented with 5% heat-inactivated FCS, 2 g l^{-1} sodium bicarbonate, 100 U ml^{-1} penicillin, and 100 μg ml^{-1} streptomycin. Cells were passaged (1:6) when they reached 80–90% confluency.

2.2. Membrane preparation

J774 cells were grown to confluence and harvested using a rubber cell scraper. Cells were suspended in PBS and centrifuged at 3000 rpm for 2 min. This process was repeated a further two times to remove any trace of growth medium. The resulting cell pellet was suspended in buffer, containing 10 mM Hepes, 1 mM EDTA, 0.5 mM phenylmethylsulfonyl fluoride (PMSF) and 6.25×10^3 IU/l Aprotinin (pH 7.4) and homogenised using an Ultra Turrax homogenizer (Janke & Kunkel, FRG) at half speed for 60 s. Homogenates were centrifuged for 10 min at 3000 rpm and the supernatant re-centrifuged at 13,000 rpm for 30 min. The pellet was resuspended in the same buffer and high-speed centrifugation repeated. The resulting pellet was resuspended to give a final protein concentration of 2–3 mg ml^{-1}, determined using the Bradford method [27]. All steps were performed at 4 °C.

2.3. Preparation of macrophages from spleen and peritoneum

Breeding, maintenance and killing of the mice used in this study followed the principles of good laboratory animal care and experimentation and complied with British Home Office and local ethical committee regulations. Mice were kept at a constant 12 h/12 h light–dark cycle with free access to food and water. This study was carried out with adult male Balb/c mice at 20 weeks. Mice were killed by exposure to an increasing dose of carbon dioxide. Death was confirmed by cervical dislocation.

Mouse peritoneal macrophages were obtained by lavage of the intraperitoneal cavity with cold balanced salt solution (BSS). For splenic macrophages, spleens were collected from mice, cells gently removed by mechanical dissociation and re-suspended in BSS. The erythrocytes were removed and mononuclear cells enriched by centrifugation on a Ficoll density gradient Histopaque 1083 (Sigma St. Louis, MO, USA). Cell viability following this procedure was over 95% in all cases, as measured by Trypan blue exclusion. The enriched mononuclear cells were adjusted to 5×10^6 cells ml^{-1} in culture medium (see above) and plated in 35 mm petri dishes. After 1 h of incubation at 37 °C in a 5% CO_2 humidified atmosphere, non-adherent cells were removed by vigorous washing and the adherent cells (approximately 10% of the original plated suspension) were maintained in culture for 24–48 h until use.

For flow cytometry experiments, fresh enriched mononuclear populations were used directly prior to the adhesion step.

2.4. Immunofluorescence

Spleen macrophages were prepared as described above and plated in 8-well LAB-TEC slides (Nalge Nunc Inter, Naperville, UK) or 12 well plates (Corning USA) for 24–48 h before immunostaining. Cells were fixed for 10 min at room temperature in 4% paraformaldehyde (BDH Labora-

tory Supply, UK) prepared in PBS. Blocking of non-specific binding sites was achieved by preincubation with normal horse serum (NHS; Harlan Sera-Lab, UK) in PBS, containing 0.05% Merthiolate (Sigma) at room temperature for 20 min, as described in detail by Llewellyn-Smith [28].

An indirect immunofluorescence method with three layer amplification was used. Antibodies against $P2X_{1-7}$, $P2Y_1$, $P2Y_2$, and $P2Y_4$ receptors raised in rabbit were allowed to react with biotinylated donkey anti-rabbit IgG secondary antibody (Jackson Immunoresearch, PA, USA) and detected with either Oregon green- or Texas Red-coupled avidin (Sigma). The P2X antibodies were obtained from Roche Bioscience (Palo Alto, CA, USA). P2X subtype-selective antibodies were each raised in rabbits against a specific 15 amino acid residue at the carboxy-terminus of each P2X receptor molecule [29]. The $P2Y_1$, $P2Y_2$, and $P2Y_4$ antibodies were obtained from Alomone (Alomone Labs. Ltd. Jerusalem, Israel). Briefly, the sections were incubated overnight with primary antibodies diluted to 5 and 2.5 $\mu g\ ml^{-1}$ (determined as optimal by previous titration) with 10% Normal Horse Serum (NHS) in PBS, containing 0.05% Merthiolate and 0.1% saponin. Subsequently, the sections were incubated with biotinylated donkey anti-rabbit IgG (Jackson Immunoresearch, PA, USA) diluted 1:500 in 1% NHS in PBS, containing 0.05% Merthiolate and 0.1% saponin for 30 min, followed by a 1 h incubation with ExtrAvidin–Oregon green or Texas Red (Sigma), both at a concentration of 1:100. In some experiments, a directly labelled, donkey anti-rabbit IgG Cy3 (Jackson Immunoresearch, PA, USA) secondary antibody was applied at a concentration of 1:100 for 1 h. All incubations were carried out at room temperature and separated by three 5 min washes in PBS. Control experiments were performed using an excess of the appropriate homologue peptide antigen to absorb the primary antibodies, and thus, confirm specific immunoreaction. The slides were visualised using a Zeiss Axioplan microscope (Zeiss, Germany), and an Edge True-View 3D fluorescence microscope (Edge Scientific Instruments, Santa Monica, CA, USA). Images were prepared with Zeiss Axioplan microscopes coupled with a Leica DC 200 image acquisition system (Leica, Cambridge, UK). The figures were prepared using the Adobe Photoshop 5.0 program.

2.5. Flow cytometry assays

Spleen cells were adjusted to 10^6 cells/sample, washed twice with BSS and incubated with BSS, containing 5% normal goat serum (NGS), on ice, for 20 min. Mouse cells were then incubated with FITC-conjugated rat anti-mouse CD3 (1:100; Serotec, UK), FITC-conjugated rat anti-mouse B220 (1:100; Serotec, UK) or FITC-conjugated rat anti-mouse F4/80 (10 μl antibody/10^6 cells; Serotec, UK) to stain T lymphocytes, B lymphocytes and macrophages, respectively, for 30 min. Samples were then washed and fixed in fresh 4% paraformaldayde (Sigma) for 10 min on ice and then extensively washed in cold BSS. The rabbit anti-rat $P2X_{1-7}$ antibodies (Roche Bioscience, Palo Alto, CA, USA) and $P2Y_1$, $P2Y_2$, and $P2Y_4$ antibodies (Alomone Labs. Ltd. Jerusalem, Israel) were diluted in BSS, 0.1% saponin medium and applied to the samples at a concentration of 0.1 μg/1 × 10^6 cells overnight at 4 °C. The samples were then washed 3 times in BSS and incubated with PE-goat anti-rabbit monoclonal antibody (Caltag Lab. Burlingame, CA, USA) at a concentration of 1 μg/10^6 cells for 30 min. The cells were then washed three times in BSS, re-suspended in PBS and analyzed on a Becton Dickinson FACSCalibur flow cytometer (San Jose, CA, USA). Negative control experiments were performed by preabsorbing the P2X and P2Y receptor antibodies with their appropriate homologue peptide antigens and/or by omission of the primary P2X or P2Y antibodies. Cells were initially gated by forward and side scatter and then by cell type-specific antibodies for macrophages ($CD11b^+$)/(F4/80) or lymphocytes ($CD3^+$) ($B220^+$).

2.6. Western blot analysis

J774 cell membrane preparations (15 μg protein) were subjected to a variety of denaturing or reducing conditions. Samples were solubilized in Laemmli sample buffer, containing 2% (w/v) sodium dodecyl sulphate (SDS) and heated for 5 min at 95 °C or in sample buffer with the addition of 3% (w/v) DTT or 5% (v/v) mercaptoethanol, both with and without heating for 5 min at 95 °C. Samples were then electrophoresed on a 10% SDS polyacrylamide gel using 25 mM Tris, 192 mM glycine and 0.1% (w/v) SDS running buffer (pH 8.3) (Biorad, Hertfordshire, UK) at 20 mAmps per gel. The proteins were transferred to nitrocellulose membranes by electrophoretic blotting for 1 h at a constant current of 1 mA/cm^2 (trans-blot semi-dry transfer cell, Biorad, Hertfordshire, UK) using transfer buffer, containing 10% (v/v) methanol, 25 mM Tris, 192 mM glycine and 0.1% (w/v) SDS (pH 8.2–8.4). Non-specific protein-binding sites were blocked with PBS-T (phosphate buffered saline (pH7.4), containing 0.1% Tween 20) and 6% (w/v) fat-free milk powder for 1 h at room temperature. The membranes were incubated with a variety of P2X (Roche Biosciences, Palo Atto, CA) or P2Y (Alomone Lab. Ltd, Jerusalem, Israel) antibodies using a 1:1000 dilution in PBS-T for 16 h at 4 °C. The membranes were then washed (2 min × 15 min) with PBS and incubated with a swine anti-rabbit IgG antibody conjugated to horseradish peroxidase (1:2000 dilution) (Amersham Pharmacia Biotech UK Limited, Bucks, UK) for 1 h at room temperature and finally washed again with PBS-T (2 min × 15 min). Bound antibodies were detected using a Visualiser Western Blot Detection Kit (Upstate Cell Signalling Solutions, NY) and a Fluor-S MultiImager System (Biorad, Hertfordshire, UK).

2.7. RT-PCR analysis

Total cellular RNA was extracted from cells using Total RNA Isolation System (Promega, Southampton UK) according to the manufacturer's instructions. Three micrograms of RNA sample were digested with 3 U of amplification grade deoxyribonuclease I (Life Technologies, Paisley, UK) for 20 min at room temperature to eliminate contaminating DNA. Half of each resulting RNA sample was reverse transcribed at 42 °C using 200 ng of random primers, 400 U of Superscript II reverse transcriptase (Life Technologies, Paisley, UK) with 40 U of ribonuclease inhibitor (Rnasin; Promega, Southampton UK) in a final volume of 50 μl reaction buffer. The remaining RNA was used to prepare a control sample where reverse transcriptase was omitted. One 2 μl aliquot of each sample was used for RT-PCR analysis in a 50 μl reaction volume, containing 200–500 nM primers, 1.5 mM $MgCl_2$, 200 μM of each dNTP and 2.5 U of Taq polymerase (Qiagen, Crawley, UK).

Cycling conditions were: 94 °C for 4 min, followed by 35 cycles of 94 °C for 60 s, 58 to 63 °C for 60 s (depending on the primer set), 72 °C for 60–90 s with a final extension step of 72 °C for 7 min.

Primer sets were designed based on the available rat and mouse sequences and published data [30–32]. The sequences were as follows:

Receptors		Primer sequence	Primer position (relative to rat sequence)
$P2X_1$	Fwd	5′-TGGGTGGGTGTTTGTCTATG-3′	344–363
	Rev	5′-TGAAGTTGAAGCCTGGAGAC-3′	1064–1083
$P2X_2$	Fwd	5′-TCCATCATCACCAAAGTCAA-3′	265–284
	Rev	5′-TTGGGGTAGTGGATGCTGTT-3′	637–656
$P2X_3$	Fwd	5′-CTCCTGCCTAACCTCACCGACAAGGACATAAAGAAGTGCCGCTTC-3′	571–616
	Rev	5′-CTAGTGACCAATAGAATAGGCCCCTGAGTCTGTAGACTGCTTCTC-3′	1150–1195
$P2X_4$	Fwd	5′-ATCCTCCCCAACATCACCACGTCCTACCTCAAATCGTGCATTTACAAT-3′	612–657
	Rev	5′-TCACTCGTTCATCTCCCCCGAAAGACCCTGCTCGTAGTCTTCCAC-3′	1122–1167
$P2X_5$	Fwd	5′-GTCACTTCAGCTCCACCAATCTCT-3′	843–866
	Rev	5′-CCTCTCCAGTGTCTTGTCCTCTGC-3′	1372–1396
$P2X_6$	Fwd	5′-GCCTTAGATACCTGGGACAACACCTATTTCAAGTACTGTCTCTAC-3′	621–666
	Rev	5′-TGCACTGTTGGTAGTTGCCTTTGGGGCTCTTGCCTCTTCATACTT-3′	1092–1137
$P2X_7$	Fwd	5′-ATGCCGGCTTGCTGCAGCTGGAACGATGTCTTTCAGTATGAGACA-3′	1–45
	Rev	5′-CCAAGTCTTGTGAAAGGTACAAGAGATGTTCATACCTGGTAAGAT-3′	621–666
$P2Y_1$	Fwd	5′-ACGTCAGATGAGTACCTGCG-3′	1235–1254
	Rev	5′-CCCTGTCGTTGAAATCACAC-3′	1504–1523
$P2Y_2$	Fwd	5′-CTGGTCCGCTTTGCCCGAGATG-3′	1417–1438
	Rev	5′-TATCCTGAGTCCCTGCCAAATGAGA-3′	1703–1727
$P2Y_4$	Fwd	5′-TGTTCCACCTGGCATTGTCAG-3′	1566–1586
	Rev	5′-AAAGATTGGGCACGAGGCAG-3′	1840–1859
$P2Y_6$	Fwd	5′-TGCTTGGGTGGTATGTGGAGTC-3′	868–889
	Rev	5′-TGGAAAGGCAGGAAGCTGATAAC-3′	1206–1184

PCR products were resolved by electrophoresis in 2% agarose gels and visualised by ethidium bromide staining. The specificity of PCR products was confirmed by digestion with specific restriction enzymes and/or sequencing.

2.8. Intracellular calcium measurements

Cells plated on glass cover slips were loaded with 6 μM Fura-2-AM (Molecular Probes) for 1 h at room temperature in culture medium. The coverslips were then washed and mounted in a three-compartment superfusion chamber whose base was formed by a coverslip, containing the cells. The central chamber, containing the cells had a volume of 200 μl, and was perfused with PBS supplemented with 1 mM $CaCl_2$ at a rate of 1 ml min^{-1}. Intracellular calcium concentrations of groups of 20–40 cells were monitored

continuously at room temperature with the use of a fluorescence photometer (Photon Technology, Princeton, NJ). Fura-2 was excited alternately at 340 and 380 nm, and the emission at 510 nm was measured. The ratio measurement, which is proportional to the intracellular calcium concentration, was determined every 100 ms. The drug application was via a bolus of nucleotides by introducing 50 μM of the perfusion saline, containing five times the desired final concentration of the drug into the pre-chamber [33]. The rapid delivery of drugs as a bolus minimizes the effects of desensitization mechanisms [34]. The intervals between drug applications were a minimum of 10 min for increasing concentrations of the same drug and between fifteen to 30 min between different drugs.

2.9. Electrophysiology

Cells were plated at low density in 35 mm plastic culture dishes (Falcon) and maintained in culture for 2–7 days. Cultures were visualised using phase contrast at 600× magnification using an inverted microscope (Diaphot, Nikon). Culture dishes were perfused with 'extracellular solution' at room temperature, at a rate of 0.5 ml min^{-1}, while solution was applied locally to the cell of interest using a microperfusion device [35]. Recordings were carried out using the conventional whole cell patch-clamp technique [36], or the perforated patch technique [37]. Patch electrodes were fabricated from thin wall borosilicate glass capillaries (Clark Electromedical, GC 150TF) and had a resistance of 2–4 MΩ when filled with 'intracellular solution'. Membrane currents were recorded using an Axopatch 200B amplifier (Axon Instruments), displayed on a chart recorder (Gould TA240) and stored on digital audiotape using a DTR-1204 (Biologic, Claix, France) recorder for subsequent line analysis. Ramp current voltage relationships were recorded on a personal computer, using pClamp software and a Digidata 1200 interface (Axon Instruments).

Traces were acquired using Fetchex (pClamp software, Axon Instruments) and plotted using Origin (version 4.0).

2.10. Drugs and solutions

Except where modified as indicated, the extracellular solution contained (mM): NaCl, 154; KCl, 4.7; HEPES, 10; D-glucose, 5.6; $CaCl_2$ and $MgCl_2$, 1.2, adjusted to pH 7.4 with NaOH. In experiments investigating P2X-mediated responses, the intracellular (pipette) solution contained (mM): citric acid, 56; $MgCl_2$, 3; CsCl, 20; HEPES, 40; EGTA, 0.1; TEA Cl, 10, adjusted to pH 7.2 with CsOH (total Cs^+ concentration, 170 mM). To investigate P2Y-mediated responses, the intracellular solution contained (mM): tri-potassium citrate, 56; KCl, 25; NaCl, 10; HEPES, 35; K EGTA, 0.1. For perforated patch recordings, amphotericin B (240 μg ml^{-1}) was added to the pipette solution.

2.11. Statistical analyses

All data are presented as mean ± S.E.M. Statistical comparisons were made using two-tailed Student's *t*-tests for paired and unpaired samples and ANOVA (Tukey's Multiple Comparison Test) as appropriate. Statistical significance was taken as $P < 0.05$.

3. Results

3.1. Nucleotides trigger Ca^{2+} changes in macrophages

3.1.1. Mouse peritoneal macrophages

We used micro-fluorimetry to investigate nucleotide receptors on native macrophages. ATP, ADP, UTP and UDP induced a rapid and concentration-dependent intracellular Ca^{2+} response in mouse macrophages, with a sharp increase of basal calcium (Fig. 1a–d). The cells were more sensitive to UDP treatment, with a response to doses as low as 100 nM (Fig. 1d). ATP at concentrations 1–100 μM induced calcium changes with a single peak (Fig. 1a), while at high concentrations (10–100 μM), UTP and UDP evoked a biphasic response with a fast peak followed by a slower second phase (Fig. 1c and d). The least effective nucleotide tested was ADP, with cells responding only at 100 μM (Fig. 1b). AMP and UMP did not induce any responses.

3.1.2. J774 macrophage cell line

We also examined the Ca^{2+} changes induced by nucleotides in the J774 macrophage cell line. We observed that ATP, ADP, 2Me-S-ATP, UTP, and UDP all elicit Ca^{2+} response at a concentration of 100 μM. In one of three experiments the J774 macrophages responded at two concentrations of a $P2X_1$ and $P2X_3$ agonist α, β-meATP but stopped responding when a higher concentration was tested (Fig. 2a). Concentration-response curves were constructed for different P2 agonists on the J774 macrophage cell line. However, in some experiments, the concentration dependence was very steep giving rise to "all or none" type responses, similar to those observed in rat alveolar macrophages [26]. Thus, combining data from different experiments gave rise to either steep concentration-response curves, or large error bars. The J774 macrophages responded consistently to a $P2Y_2$ agonist UTP (EC_{50} = 0.9 μM) (Fig. 2b), $P2Y_6$ agonist UDP (EC_{50} = 25 μM) (Fig. 2c), and $P2Y_1$ agonists ADP (EC_{50} = 11.5 μM) and 2Me-S-ADP (EC_{50} = 3.9 μM) (Fig. 2d and e), respectively.

3.2. Patch-clamp studies in J774 cells

We used whole cell patch-clamp recording to further characterize the P2 receptors present on J774 cells. This has the advantage of readily discriminating between responses mediated by P2X or P2Y receptors. It also

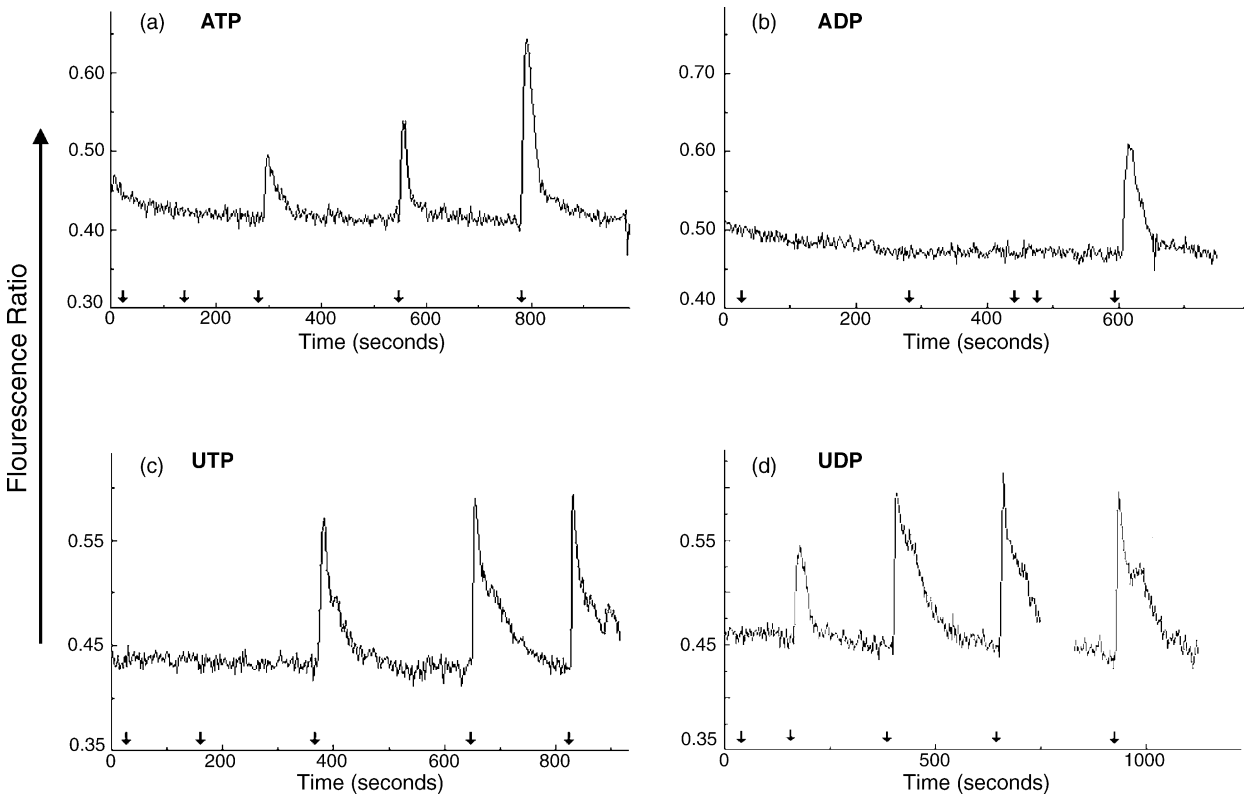

Fig. 1. Effect of extracellular nucleotides on intracellular calcium concentration in mouse peritoneal macrophages. Murine macrophages were loaded with Fura-2, and nucleotides at a final concentration of 10 nM, 100 nM, 1 μM, 10 μM or 100 μM were added rapidly (arrows). (a) ATP response. (b) ADP response. (c) UTP response. (d) UDP response. The reagent concentration in the chamber decreased to zero within 1 min due to continuous perfusion of the extracellular medium. Fluorescence is proportional to the intracellular calcium concentration and was measured as described in Section 2. Representative data of a single experiment are shown. The experiments were repeated at least three times with similar results.

permits the use of antagonists, such as PPADS and Cibacron blue, which because of their colour, interfere with fluorimetric measurements.

3.2.1. P2Y receptors

Most cells (24/28) voltage clamped at −45 mV, with a K^+ based internal solution, responded to ATP with a slowly developing outward current (Fig. 3a). When recorded with the conventional whole cell recording technique, the response exhibited pronounced run-down, such that only one or two responses could be obtained from each cell. In contrast, when the perforated patch technique was employed, reproducible responses could be obtained. The reversal potential obtained for this current was $E_{rev} = -78 \pm 0.35$ mV ($n = 4$) and is compatible with the activation of a Ca^{2+}-dependent K^+ conductance that has already been described by our group in peritoneal mononuclear and polykaryon macrophages [38]. These outward currents were little changed by the selective SK_{1-3} channel blocker UCL 1648 (100 nM), but were abolished by the SK_4/IK_1 channel blocker clotrimazole (1 μM; Fig. 3b and c). UTP and UDP induced the activation of the same outward current in concentrations of 1–10 μM (Fig. 3a), but higher concentrations of ADP (30–100 μM) were required to evoke consistent responses. We investigated the concentration-dependence of the activation of this outward current by ATP, ADP, UTP and UDP. For some cells, the concentration dependence was very steep giving rise to "all or none" type responses. This resulted in large error bars, and steep curves for the pooled data (Fig. 4). Nevertheless, we have obtained EC_{50} values of 1.3, 0.9, 10.3 and 33.2 μM for UTP, UDP, ATP and ADP, respectively. We further characterized the receptors mediating this response by examining the effect of four different antagonists, which have varying degrees of selectivity between different P2Y receptor subtypes. Cibacron blue (10 μM) produced a reversible inhibition of the response to UDP, UTP and ADP (Fig. 5a), while suramin (100 μM) blocked the response to ADP but did not affect the response to UTP (Fig. 5b). PPADS (30 μM) produced a slowly reversible block of the response to ADP, and although the response to UTP was also reduced, the effect was less pronounced than the effect against ADP (Fig. 5c). The $P2Y_1$ selective antagonist MRS 2179 at a concentration of 3 μM failed to alter the response to either ADP or UTP (Fig. 5d).

3.2.2. P2X receptors

In cells voltage, clamped at −60 mV, with a Cs^+ based internal solution (to block K^+ currents), ATP (100 μM) evoked a small (≤100 pA), rapidly activating inward cur-

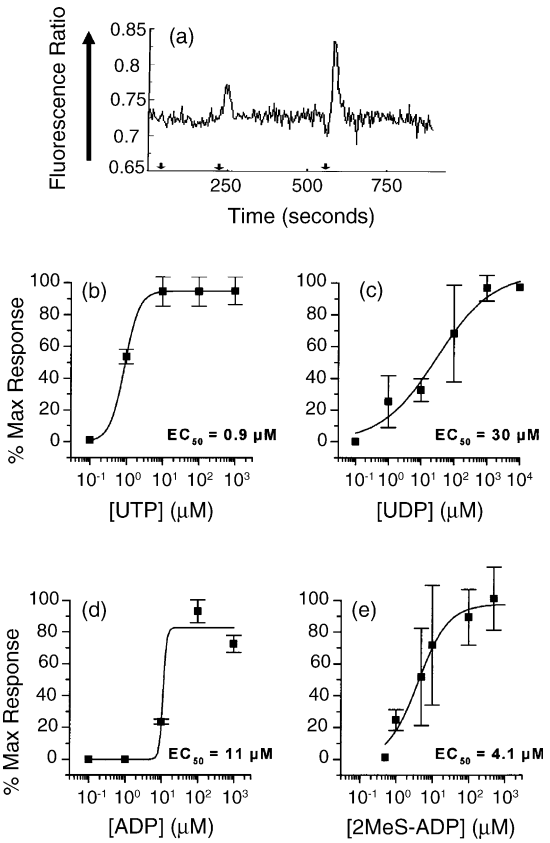

Fig. 2. Concentration-dependent elevation of intracellular Ca^{2+} by nucleotides in J774 macrophages. (a) Calcium mobilization in response to increasing concentration of α, β-meATP (arrows represent 0.1 μM, 1 μM and 10 μM). Subsequent application of higher concentrations of agonist failed to evoke responses (not shown). (b–e) Show concentration-response curves for Ca^{2+} mobilization in response to the increasing concentrations of UTP, UDP, ADP and 2Me-S-ADP respectively. Concentration-response curves were generated by combining data from at least three independent experiments.

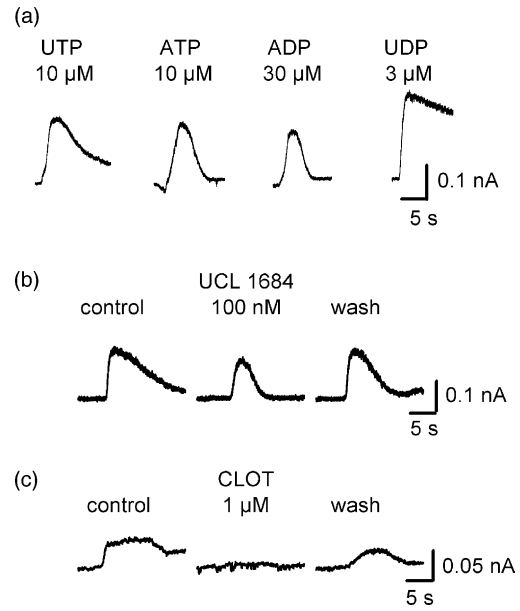

Fig. 3. Nucleotide activation of outward currents in J774 cells under voltage clamp. (a) Outward currents evoked by UTP, ATP, ADP and UDP in the same cell, under voltage clamp at −45 mV, using the perforated patch technique with a K^+ based filling solution. (b) The selective SK channel blocker UCL 1684 has little effect on the outward current. (c) recordings from another cell, in which, the response was reversibly abolished by the IK channel blocker clotrimazole (CLOT).

rent, which declined during the course of a 2 s application (Fig. 6a). In contrast, the $P2X_1$- and $P2X_3$- selective agonist α, β-meATP (30 μM) failed to evoke any inward current, even when cells had been pre-incubated with apyrase (4 U ml^{-1}) for more than 2 h, to prevent receptor desensitisation by any endogenously released ATP (data not shown).

Di-benzoyl-ATP is more potent than ATP on the $P2X_7$ receptor (24). In "normal" divalent cation-containing solution, this agonist produced a much smaller response than ATP (Fig. 6a center trace), but when the divalent cation concentration was reduced (to 0.5 mM Ca^{2+}, 0 mM Mg^{2+}), the response to BzATP was much greater than that to the same concentration of ATP (Fig. 6a lower right trace and 6b).

The response to ATP, recorded in normal divalent cation solution, was concentration-dependent, and fitting the Hill equation to the data gave an EC_{50} of 11 μM (Fig. 7a).

The response to 10 μM ATP, recorded in normal divalent cation solution was potentiated in the presence of 10 μM Zn^{2+}, but was attenuated when the pH was lowered from 7.4 to 6.8 (Fig. 7b and c).

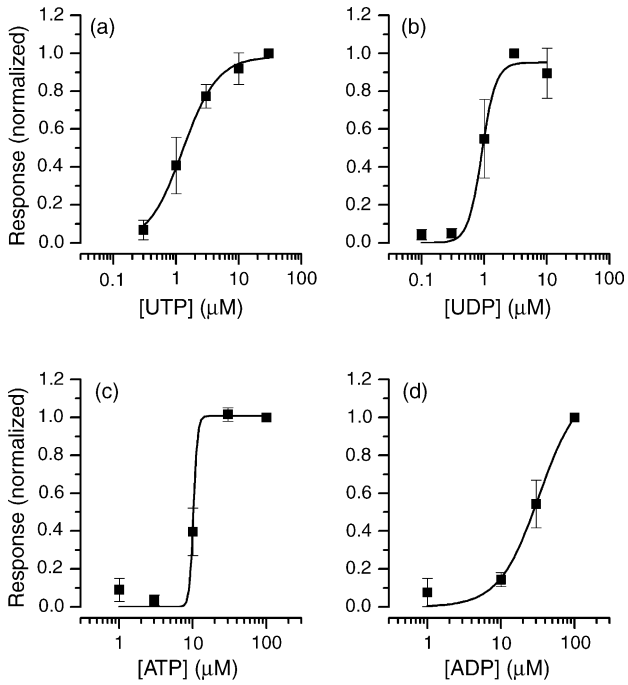

Fig. 4. Concentration-dependence for activation of outward currents in J774 cells under voltage clamp. Graphs show the concentration-response curves for UTP, UDP, ATP and ADP. Responses were normalized with respect to that produced by 3 μM (UDP) or 100 μM (UTP, ATP, ADP) agonist in the same cell. The Hill equation was then fitted to the pooled data to determine an EC_{50} value. Points represent the mean from 4 to 8 cells.

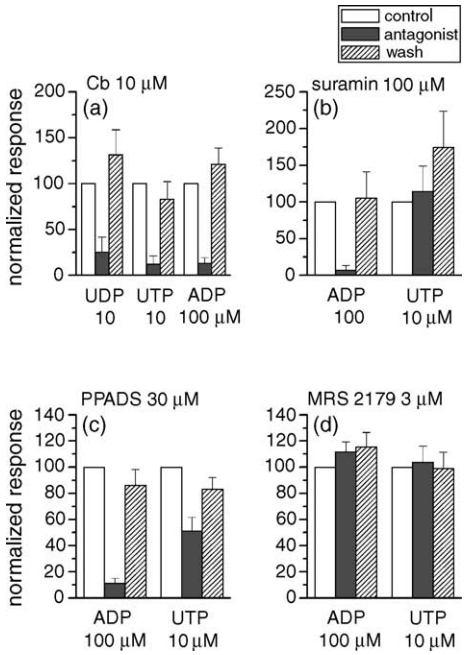

Fig. 5. Antagonist sensitivity of nucleotide activated outward currents under voltage clamp. (a) Comparison of responses to near maximal agonist concentrations of UDP, UTP and ADP before, during and after application of Cibacron blue. (b) Comparison of responses to near maximal concentrations of ADP and UTP before, during and after application of 100 μM suramin. (c) Comparison of responses to ADP and UTP before, during and after application of 30 μM PPADS. (d) Failure of the $P2Y_1$ selective antagonist MRS 2179 (3 μM) to affect responses to ADP and UTP. Responses amplitudes were normalized with respect to the control response in each cell. Columns represent the mean from six cells.

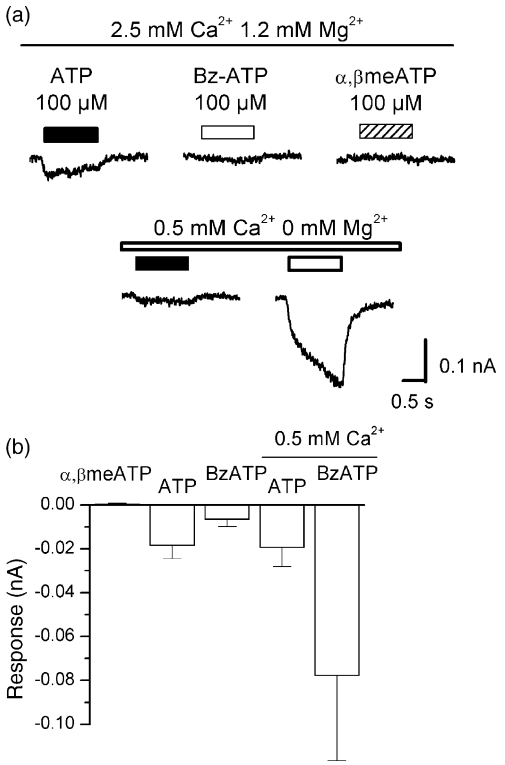

Fig. 6. Agonist activated inward currents in voltage clamped J774 cells. (a) Rapid application of ATP evokes an inward current in cells voltage clamped at −60 mV with a Cs^+ based internal solution. In contrast, BzATP evoked a much smaller response, and no response was evoked by α, β-meATP. When the divalent cation concentrations in the bathing solution were reduced, the response to BzATP was greatly increased. (b) Comparison of the amplitude of the inward current produced by ATP, BzATP and α, β-meATP in normal bathing solution, and by ATP and BzATP in low divalent cation-containing solution (0 mM Mg^{2+}, 0.5 mM Ca^{2+}). Columns represent the mean ± S.E.M. from eight cells.

The P2 antagonists suramin (100 μM) and Cibacron blue (30 μM) failed to antagonise the response to ATP in normal divalent cation solution (Fig. 7d). In fact, suramin appeared to produce a small though not statistically significant potentiation of the response.

3.3. Immunostaining for P2X receptors in the J774 macrophage cell line

We investigated the expression of all seven P2X receptor subunits in J774 cells using immunofluorescence. Positive immunostaining was observed for all P2X receptors with different intensities of staining (Fig. 8a–h). In most experiments, $P2X_7$, $P2X_4$ and $P2X_3$ receptor immunostaining was stronger than for other P2X receptor subtypes, with staining intensity varying from weak to strong for all P2X subtypes. The majority of cells were weakly labelled with the anti-$P2X_1$ and -$P2X_2$ receptor antibodies (Fig. 8a and b). The intensity of immunostaining was similar for $P2X_4$, $P2X_3$ and $P2X_7$ receptors, with the majority of cells strongly labelled and some with moderate staining intensity (Fig. 1c, d and h). $P2X_5$ and $P2X_6$ immunostaining was also variable; less than half the cell population examined showed strong staining, while the majority of cells were moderate to weakly stained (Fig. 8e and f). The negative controls (pre-absorption with cognate peptide, or omission of the primary antibodies) gave no staining for any of the P2X receptors studied. The negative control for $P2X_6$ is shown in Fig. 8g. In general, we observed the following order of staining intensity: $P2X_4 \geq P2X_7 \geq P2X_3 > P2X_6 \geq P2X_5 \gg P2X_2 > P2X_1$.

3.4. Western blot analysis

Western blotting was performed on membrane samples subjected to a variety of denaturing or reducing conditions (Section 2) using antibodies raised against $P2X_{1-7}$ receptors. J774 cells were found to express $P2X_4$, which was detectable when the sample was treated with DTT or mercaptoethanol and $P2X_7$, which was only detectable following reduction with DTT (Fig. 9). In both instances, further denaturing of the protein by heating at 95 °C abolished the ability of the antibody to detect the protein. These proteins were detected at 60 and 70 kDa for $P2X_4$ and $P2X_7$, respectively, which corresponds to the known molecular weight of these proteins. No protein for $P2X_1$, $P2X_3$ $P2X_5$ or $P2X_6$ could be detected, while a weak band at 70 kD was detected for $P2X_2$. Staining for $P2X_2$, $P2X_4$

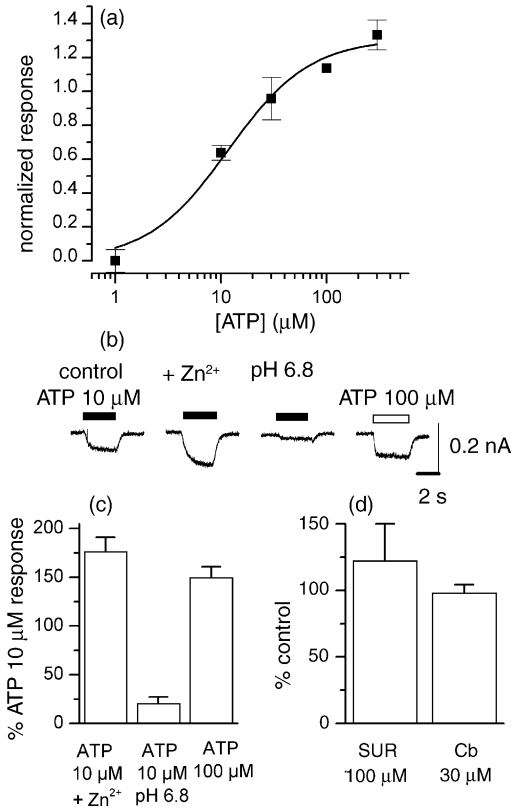

Fig. 7. Pharmacological properties of the ATP-activated current (in normal divalent cation solution) in voltage clamped J774 macrophages. (a) concentration-response curve for activation of the inward current by ATP. Points represent the mean ± S.E.M. from four cells. Fitting the Hill equation to the data gave an EC_{50} of 11 μM. (b) Inward currents recorded from the same cell in response to 10 μM ATP alone, in the presence of 10 μM Zn^{2+}, or in solution at pH 6.8 compared with a response to 100 μM ATP. (c) Comparison of the effects of Zn^{2+} and low pH on the response to ATP. Columns represent the mean ± S.E.M. from eight cells. (d) Comparison of the effects of suramin (SUR 100 μM) and Cibacron blue (CB 30 μM) on the response to 10 μM ATP. Columns represent the mean ± S.E.M. from four cells.

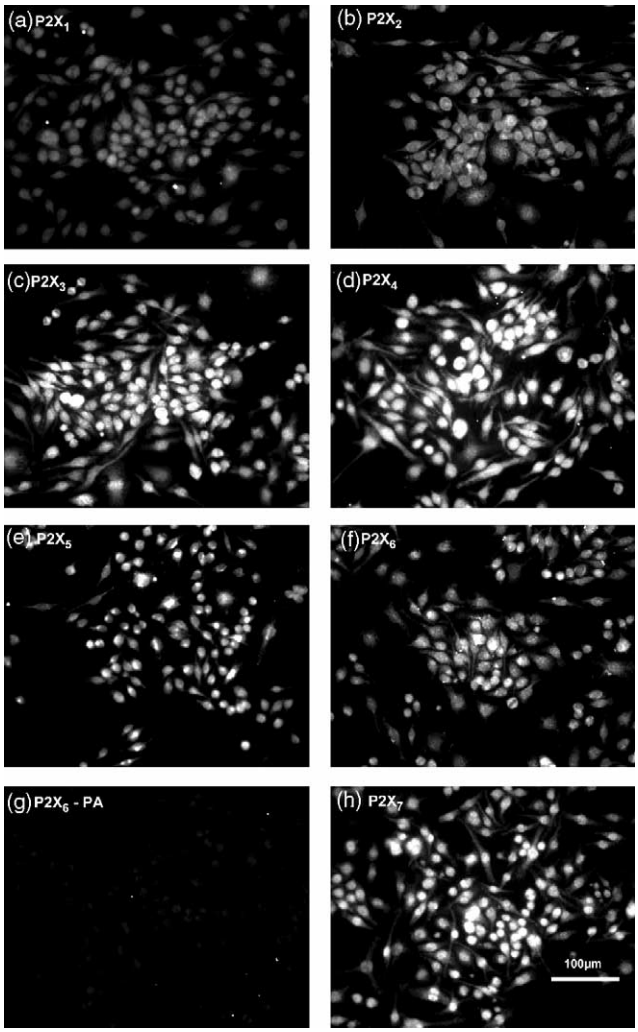

Fig. 8. Immunolabelling of P2X receptors on J774 macrophages. Immunofluorescent staining of: (a) $P2X_1$ (b) $P2X_2$ (c) $P2X_3$ (d) $P2X_4$ (e) $P2X_5$ (f) $P2X_6$ (g) pre-absorption of $P2X_6$ antibody with peptide control. (h) $P2X_7$ immunofluorescence. Note that there is less intense immunoreactivity for $P2X_1$ and $P2X_2$ than for other receptors. (a–h) 200×.

and $P2X_7$ was abolished by pre-absorption with the cognate peptide (not shown).

3.5. Immunostaining for P2Y receptors in the J774 macrophage cell line

We studied the expression of $P2Y_1$, $P2Y_2$ and $P2Y_4$ receptors by immunofluorescence. The J774 macrophages were positively-immunostained for all of these receptors (Fig. 10a–d). Immunolabeling was strongest for $P2Y_1$ receptors followed by $P2Y_2$ and $P2Y_4$. The majority of J774 cells were strongly stained with anti-$P2Y_1$ antibodies but some cells presented a moderate intensity of labeling (Fig. 10a). The anti-$P2Y_2$ receptor antibody labeled approximately half of the J774 macrophage population, with moderate to strong staining intensity (Fig. 10c). The majority of cells were moderately stained for $P2Y_4$, with some strong staining observed (Fig. 10d). In some experiments, $P2Y_1$ receptor immunostaining was more concen-

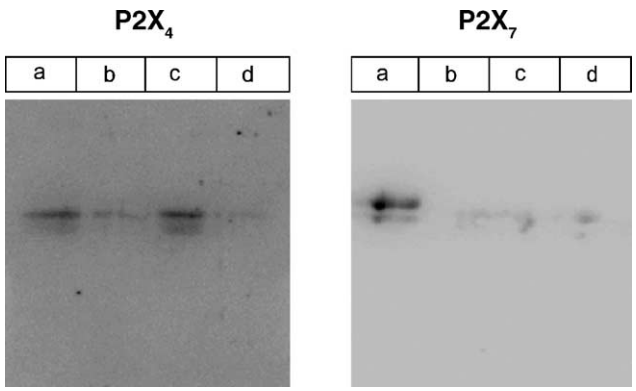

Fig. 9. Detection of $P2X_4$ and $P2X_7$ in J774 membrane preparations by western blotting. Samples were treated with Laemmli buffer, containing (a) 3% DTT, (b) 3% DTT with heating at 95 °C (c) 5% mercaptoethanol and (d) 5% mercaptoethanol with heating at 95 °C. Proteins of 60 and 70 kDa were detected for $P2X_4$ and $P2X_7$, respectively.

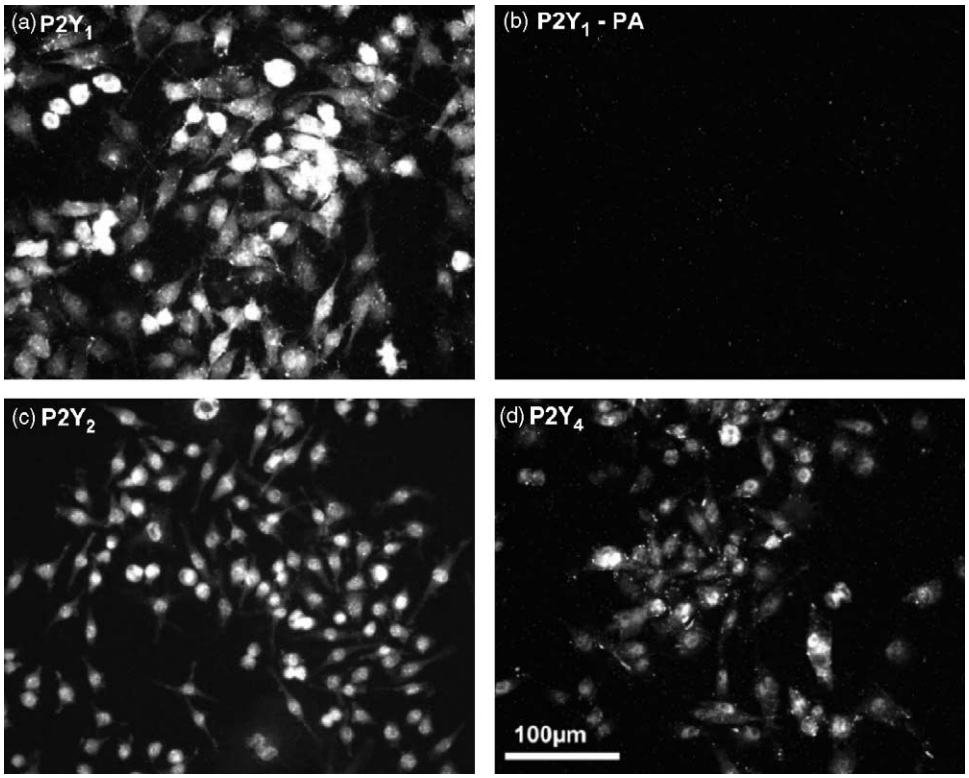

Fig. 10. Immunolabelling of P2Y receptors on J774 macrophages. (a) $P2Y_1$ immunofluorescence staining. (b) Pre-absorption of $P2Y_1$ antibody with peptide control. (c) $P2Y_2$ immunoreactivity. (d) $P2Y_4$ immunoreactivity. *Note*: In (a), the presence of a subpopulation of cells that label strongly for $P2Y_1$ receptors. (a–d) 200×.

trated on the plasma membrane than that observed for other P2Y receptors. The negative controls gave no staining for any of the P2Y receptors studied.

3.6. P2X receptor expression in mouse spleen macrophages

Using flow cytometry, we assessed the expression of P2X receptors in mouse spleen macrophages. No significant immunoreactivity for $P2X_1$ or $P2X_2$ was observed. A weak signal for $P2X_3$ was apparent, while strong immunoreactivity for the other four subunits was detected (Fig. 11; Table 1). All P2X receptor subtypes were identified in spleen macrophages but the mean fluorescence intensity (MFI: an index of receptor number per cell) sometimes showed weaker expression of $P2X_1$ and $P2X_2$ receptor subtypes (Table 1).

3.7. P2Y receptor expression in mouse spleen macrophages

Using flow cytometry, we assessed the expression of $P2Y_1$, $P2Y_2$ and $P2Y_4$ receptors in mouse spleen macrophages. All three P2Y receptor subtypes were identified with little difference in the mean fluorescence intensity between the subtypes (Table 1). For the established macrophage cell line J774, we used conventional immunostaining.

3.8. Molecular analyses of P2X and P2Y receptors

We used RT-PCR to identify mRNA expression corresponding to specific receptors found in mouse spleen macrophages and in the J774 macrophage cell line. Amplifications were performed with the oligonucleotide primer pairs specific for cloned P2X and P2Y receptors. Primers were complementary to regions showing maximal sequence identity within mouse and rat transcripts (where both sequences were available). The results are summarised in Fig. 12 and Tables 1 and 2.

Single, specific PCR fragments were detected for $P2X_4$ and $P2X_7$ in spleen and peritoneal macrophages as well as in J774 cells. In mouse macrophages, two fragments were amplified for $P2X_6$; a fragment of the expected size and a smaller, less abundant one. Sub-cloning and sequence analysis of this smaller product indicated that it arises from alternative splicing of the mouse $P2X_6$ transcript.

Amplification of $P2X_3$ mRNA resulted in two fragments, one of the expected size and a second smaller band of higher intensity. However, sequence analysis revealed that the smaller fragment is a non-specific product of PCR amplification.

Amplification with primer sets specific for $P2X_1$ and $P2X_5$ gave specific products of low abundance in isolated macrophages but were largely undetectable in J774 cells. $P2X_2$ amplification produced a single band of a much larger size (800 bp) than expected (392 bp). This fragment

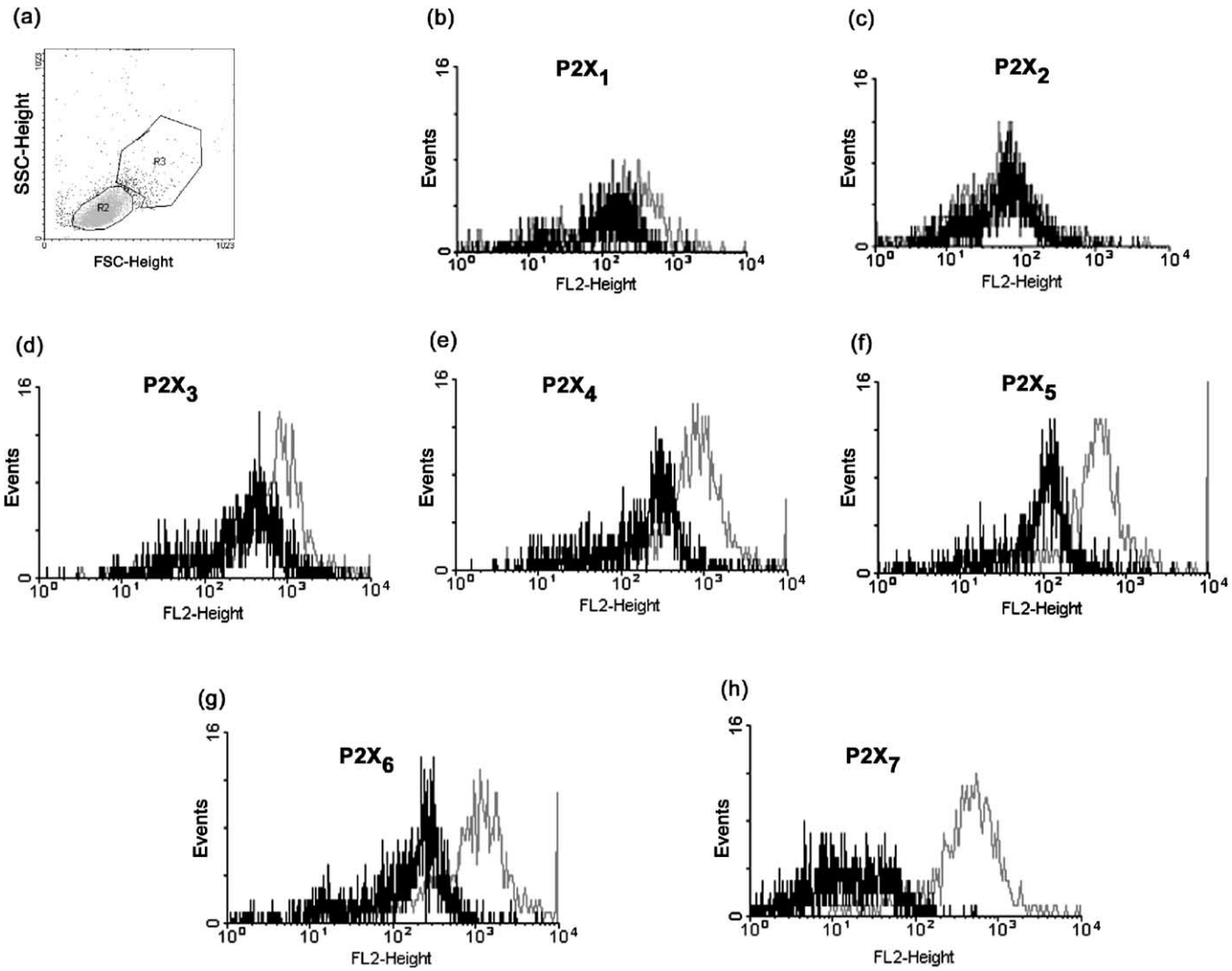

Fig. 11. P2X receptor subtype protein expression in spleen macrophages using flow cytometry. Fluorescence histograms of P2X receptors obtained by flow cytometry. (a) Cells were initially selected for analysis on the basis of the characteristic forward (*x*-axis) and side (*y*-axis) scatter profiles; cells in region R3 were gated to represent the macrophage population (R2 consisted mainly of lymphocytes). These cells were confirmed to be CD11b-positive (a marker for macrophages). (b) $P2X_1$ (c) $P2X_2$ (d) $P2X_3$ (e) $P2X_4$ (f) $P2X_5$ (g) $P2X_6$ (h) $P2X_7$. Solid line, control; shaded line, P2X subtype antibodies. Traces shown are from a single experiment but are representative of five independent experiments.

corresponded to the published sequence of the genomic DNA. However, this amplicon was not detected in control amplifications with mock first strands where reverse transcriptase was omitted, thus excluding genomic DNA contamination. Therefore, we have amplified the unspliced, primary transcript of the $P2X_2$ receptor, retaining introns between exon 2 and exon 6. Furthermore, we did not observe the amplification product of the mature, spliced mRNA, which indicates that the $P2X_2$ transcript in macrophages is alternatively spliced in the region(s) where the amplification primer(s) anneal. Sequence analysis revealed that exon 6 (to which our reverse primer should anneal) undergoes extensive splicing in different tissues. Amplification with primer sets specific for $P2Y_1$, $P2Y_2$, $P2Y_4$ and $P2Y_6$ transcripts resulted in single amplification products of the expected sizes in isolated macrophages and in the

Table 1
Summary of P2X receptor subtypes identified in macrophages by RT-PCR and immunocytochemistry

	$P2X_1$			$P2X_2$			$P2X_3$			$P2X_4$			$P2X_5$			$P2X_6$			$P2X_7$		
	P	IS	WB	P	IS	WB	P	IS	WB	P	IS	WB	P	IS	WB	P	IS	WB	P	IS	WB
J774 cell line	–	±	–		+	+	+	++	–	+	+++	++	±	+	–	+	+	–	+	+++	++
Mouse spleen macrophages	NE	++ (var)	NE	NE	++ (var)	NE	+	++	NE	+	+++	NE	+	+	NE	+	++	NE	+	++	NE

P, RT-PCR; IS, Immunostaining (immunofluorescence or flow cytometry data); WB, Western blot; (–) not detected; (+) staining present; (++) strong staining; (+++) very strong staining; (var), variable; NE not examined.

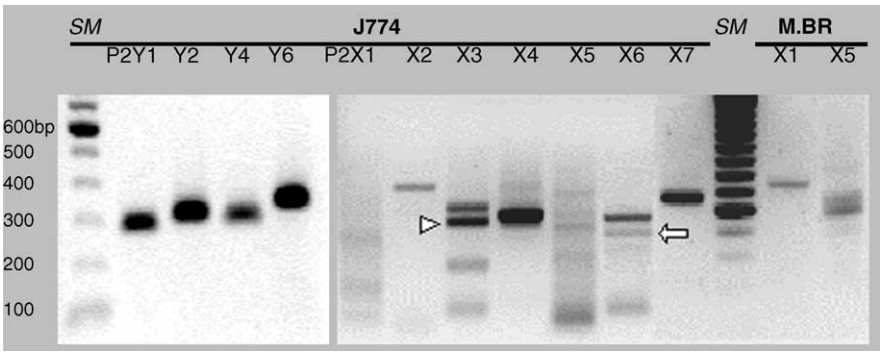

Fig. 12. RT-PCR determination of purinergic receptor mRNA expression in mouse macrophages. The figure shows examples of agarose gel analysis (negative image of the ethidium bromide staining) of 10 μl of amplification products obtained with specific primer sets. J774—mouse macrophage cell line; SM—100 bp size marker (control; Gibco-BRL). The initial identification of the PCR products was based on the correct predicted size and confirmed by restriction digestion and/or sequencing. The single, expected size amplification products were obtained for all P2Y receptors studied and for $P2X_4$ and $P2X_7$. Amplification of $P2X_6$ gave an additional smaller band (arrow) proven to be the result of alternative splicing. A larger band in $P2X_3$ (arrowhead) was a non-specific product. The size of $P2X_2$ amplicon corresponded to the amplification of an unspliced, primary transcript. Although no amplification product for $P2X_1$ and $P2X_5$ could be detected form J774 cells, amplification of products from mouse brain RNA (M.BR) served as a positive control.

J774 cell line. PCR using control first strands (prepared without reverse transcriptase) invariably gave no amplification products.

4. Discussion

In earlier studies, it was thought that $P2X_7$ and $P2Y_2$ were the main P2 receptors expressed by immune cells ([16,38,39]). Subsequent studies, using RT-PCR and immunohistochemistry, have now identified various other P2X and P2Y subtypes in immune cells [39], including lymphocytes [22], dendritic cells [25], eosinophils [40] and human blood-derived macrophages [24]. In this study, we demonstrate that mouse macrophages express a number of functional P2 receptors. Using RT-PCR and immunohistochemical techniques (immunofluorescence and Western blot for J774 cells, or flow cytometry for native macrophages), we show for the first time, both at the mRNA and protein level, that murine macrophages express both the mRNA and protein for multiple P2X receptor subunits and four P2Y receptor subtypes. Furthermore, the presence of a variety of P2X and P2Y receptor subtypes is confirmed by our functional studies.

Table 2
Summary of P2Y receptor subtypes identified in macrophages by RT-PCR and immunocytochemistry

	$P2Y_1$		$P2Y_2$		$P2Y_4$		$P2Y_6$	
	P	IS	P	IS	P	IS	P	IS
J774 Cell Line	+	+++	+	++	+	+	+	NE
Mouse spleen macrophages	NE	+	NE	+	NE	+	NE	NE

P, RT-PCR; IS, immunostaining (immunofluorescence or flow cytometry data); (–) not detected; (+) staining present; (++) strong staining; (+++) very strong staining; NE, not examined.

4.1. P2X receptors on J774 cells

Previous studies measuring $[Ca^{2+}]_i$ support the view that P2X and P2Y receptors are present on J774 macrophage cells [13,14]. Our patch-clamp and RT-PCR experiments revealed the presence of several P2X receptor subtypes on J774 macrophage cells. Our results in ''normal'' divalent cation-containing solution, revealed BzATP to be a less potent agonist than ATP, and responses were insensitive to the antagonists suramin and Cibacron blue. In addition, although responses were potentiated by micromolar concentrations of Zn^{2+}, they were attenuated by acidification. These findings are consistent with the involvement of $P2X_4$ receptors, which have been identified in a rat alveolar macrophage cell line [26]. In low divalent cation solution, BzATP became more potent than ATP indicating the presence of $P2X_7$ receptors. Our electrophysiological and pharmacological findings are supported by the strong immunostaining for $P2X_4$ and $P2X_7$ receptor protein in these cells, detection of the protein by Western blot, and the identification of mRNA for these subunits by RT-PCR.

The presence of $P2X_1$ receptor expression in immune cells is contentious. $P2X_1$ receptor mRNA and positive immunostaining were first described in thymocytes [23,41,42], and $P2X_1$ receptor mRNA has been identified in human blood-derived macrophages and macrophage-derived dendritic cells as well as in the HL60 promyelocyte cell line [43,44]. However, these findings are in contrast to a study where expression of the $P2X_1$ receptor was identified in human platelets but not in monocytes, neutrophils or blood lymphocytes [45]. We failed to detect $P2X_1$ mRNA, in J774 cells, and although low levels of $P2X_1$ immunoreactivity were detected, this was not confirmed by Western blot, so we cannot completely rule out the possibility that this was non-specific. Although no immunoreactivity was detected in our negative controls, because of the high levels

of Fc receptors on macrophages, some non-specific binding of the primary antibody might still occur. Absence of $P2X_1$ receptors is also supported by the lack of response to α, β-meATP in our patch-clamp experiments.

Although we detected low levels of $P2X_2$ receptor immunoreactivity in J774 cells by immunostaining and Western blot, our PCR experiments gave ambiguous results, possibly because of alternative splicing of the mRNA in the region to which our primers were directed. Furthermore, in our patch-clamp experiments, ATP responses were not potentiated by lowering pH, which is a characteristic of the $P2X_2$ receptor.

The detection of $P2X_3$ mRNA and protein in J774 cells was an unexpected finding as previous studies have reported selective expression of $P2X_3$ receptors largely on sensory neurones of dorsal root, trigeminal and nodose ganglia [46,47], although more recently $P2X_3$ receptors have also been identified in endothelial and epithelial cells [18,23]. Although immunostaining indicated the presence of $P2X_3$ protein, this was not confirmed by Western blot. Furthermore, our electrophysiological experiments failed to reveal the presence of functional $P2X_3$ receptors. It is possible that the receptor may not be transported to the surface membrane, as happens with the $P2X_6$ receptor when expressed in HEK293 cells [48]. Alternatively, because the $P2X_3$ receptor desensitizes very rapidly, the lack of electrophysiological response could be due to endogenous ATP release causing receptor inactivation prior to experimentation. However, in experiments using apyrase to degrade any released ATP, we were still unable to observe responses to α, β-meATP, making this explanation unlikely. Interestingly, we did occasionally see responses to α, β-meATP in our micro-fluorimetry experiments. Furthermore, human blood-derived macrophages respond to ATP and α, β-meATP, and this response has a rapidly desensitizing component, consistent with the involvement of $P2X_1$ or $P2X_3$ receptors [49]. Thus, it may be that functional $P2X_3$ receptors are only present in macrophages under particular conditions.

Although low levels of $P2X_5$ and $P2X_6$ receptor immunoreactivity were detected in J774 cells, mRNA for the $P2X_5$ subunit was not convincingly detected, while for the $P2X_6$ receptor both the expected size fragment and a smaller splice variant were observed. However, $P2X_6$ subunits may only form functional receptors if appropriately glycosylated [50] or in combination with other subunits as part of a heteromeric receptor [51]. Although our functional studies provide no support for the presence of either of these receptors, we cannot rule out their existence in J774 cells.

4.2. P2Y receptors on J774 cells

In agreement with previous studies [14], we demonstrated that nucleotides can cause an elevation of intracellular Ca^{2+} in J774 cells through the activation of P2Y receptors, and this in turn leads to the activation of a calcium-sensitive potassium conductance. Interestingly, the potassium channels involved appear to be of the IK/(SK_4) rather than the apamin sensitive (SK_{1-3}) subtype.

Our RT-PCR and immunohistochemical experiments indicate that $P2Y_1$, $P2Y_2$, $P2Y_4$ and $P2Y_6$ receptors are all present in J774 cells. This conflicts with the observations of Chen and Lin [15] who detected only $P2Y_6$ mRNA in J774 cells, and a more recent study of rat alveolar macrophages, which detected $P2Y_1$, $P2Y_2$, $P2Y_4$ and $P2Y_{12}$ but no $P2Y_6$ mRNA [26]. The presence of multiple P2Y receptors with different levels of receptor reserve, and the all or none nature of the Ca^{2+} increase in most J774 cells makes pharmacological identification of the receptor subtype(s) involved difficult. In addition, pharmacological characterization of recombinant mouse P2Y receptors is less complete than for the rat and human orthologues. Because, it is at present, unclear whether there is much interspecies variation in the properties of these receptors, interpretation of our data based on the characteristics of rat and human P2Y receptors must be treated with caution.

Our functional experiments (electrophysiology and micro-fluorimetry) show that ADP, ATP, UTP and UDP are all effective agonists. The rank order of potency differed in the two sets of experiments. Whether this is because the cell selection criteria for the two techniques resulted in an unavoidable bias is not clear.

The low potency of ADP, and the lack of antagonism by MRS 2179 would suggest that the $P2Y_1$ receptor is not important for the functional responses. The ability of suramin and PPADS to abolish responses to ADP, while leaving the response to UTP unaffected by suramin, or slightly reduced by PPADS, combined with the resistance of the response to UTP to both suramin and PPADS, might suggest the involvement of three P2Y receptor subtypes, perhaps $P2Y_2$, $P2Y_4$ and $P2Y_6$. Clearly, a more detailed investigation, using an assay more closely coupled to receptor activation (e.g. IP_3 generation) will be required to confirm this and to rule out any possible contribution of a lower expression level of $P2Y_1$ receptors.

4.3. Native macrophages

We examined the expression of P2 receptor mRNA and protein in mouse spleen macrophages using RT-PCR and flow cytometry. Although there may be problems in extrapolating from mRNA to protein, and from protein expression to functional receptors, our data suggests that purinergic signalling in native macrophages could involve at least as many receptor subtypes as we have identified in J774 cells.

4.4. Physiological role

The expression of a variety of different P2 receptors will enable a cell to respond to a variety of purine and pyrimidine di- and tri-phosphates over an extended concentration range. The extent to which the expression of these receptors

changes during the lifetime of a macrophage has yet to be investigated. Thus, it may be that some of these receptors have an important role in the development and differentiation of stem cells in bone marrow, while others are important for activation of mature macrophages. Further studies will be required to investigate this possibility.

In conclusion, we have demonstrated the presence of at least two P2X and three P2Y receptor subtypes in mouse macrophages. This suggests that the mechanisms by which nucleotides act on macrophages are more complex than first described and a re-evaluation of previous data may be necessary in light of our new findings. Clearly, the development of new P2X and P2Y specific antagonist/blocking drugs and new studies are required to establish fully the functions of different nucleotides on macrophages and the role of these receptors in macrophage physiology.

Acknowledgments

The authors are grateful to Dave Blundell and Vandir da Costa for their excellent technical support and to Dr. Chrystalla Orphanides for editorial assistance with the manuscript. This work was partially supported by funds from the Conselho Nacional de Desenvolvimento Cientifico e Technologico do Brasil (CNPq), Programa de Núcleos de Excelência (Pronex), Fundação de Amparo à Pesquisa do Estado do Rio de Janeiro (FAPERJ), and the Wellcome Trust. Dr. Coutinho-Silva was a Wellcome Trust fellow, number 062754/Z00Z.

References

[1] Burnstock G. The past, present and future of purine nucleotides as signalling molecules. Neuropharmacology 1997;36:1127–39.
[2] Ralevic V, Burnstock G. Receptors for purines and pyrimidines. Pharmacol Rev 1998;50:413–92.
[3] Communi D, Gonzalez NS, Detheux M, Brezillon S, Lannoy V, Parmentier M, et al. Identification of a novel human ADP receptor coupled to G(i). J Biol Chem 2001;276:41479–85.
[4] Hollopeter G, Jantzen H-M, Vincent D, Li G, England L, Ramakrishnan V, et al. Identification of the platelet ADP receptor targeted by antithrombotic drugs. Nature 2001;409:202–7.
[5] Jacobson KA, King BF, Burnstock G. Pharmacological characterization of P2 (nucleotide) receptors. Celltransmissions 2000;16:3–16.
[6] Abbracchio MP, Boeynaems JM, Barnard EA, Boyer JL, Kennedy C, Miras-Portugal MT, et al. Characterization of the UDP-glucose receptor (re-named here the P2Y14 receptor) adds diversity to the P2Y receptor family. Trends Pharmacol Sci 2003;24:52–5.
[7] Inbe H, Watanabe S, Miyawaki M, Tanabe E, Encinas JA. Identification and characterization of a cell-surface receptor, P2Y15, for AMP and adenosine. J Biol Chem 2004;279(19):19790–5.
[8] Cohn ZA, Parks E. The regulation of pinocytosis in mouse macrophages. 3. The induction of vesicle formation by nucleosides and nucleotides. J Exp Med 1967;125:457–66.
[9] Schmid-Antomarchi H, Schmid-Alliana A, Romey G, Ventura MA, Breittmayer V, Millet MA, et al. Extracellular ATP and UTP control the generation of reactive oxygen intermediates in human macrophages through the opening of a charybdotoxin-sensitive Ca^{2+}-dependent K^+ channel. J Immunol 1997;159:6209–15.
[10] Perregaux D, Gabel CA. Interleukin-1 beta maturation and release in response to ATP and nigericin. Evidence that potassium depletion mediated by these agents is a necessary and common feature of their activity. J Biol Chem 1994;269:15195–203.
[11] Solle M, Labasi J, Perregaux DG, Stam E, Petrushova N, Koller BH, et al. Altered cytokine production in mice lacking P2X(7) receptors. J Biol Chem 2001;276:125–32.
[12] Coutinho-Silva R, Perfettini JL, Persechini PM, Dautry-Varsat A, Ojcius DM. Modulation of P2Z/P2X(7) receptor activity in macrophages infected with *Chlamydia psittaci*. Am J Physiol Cell Physiol 2001;280:C81–9.
[13] Steinberg TH, Silverstein SC. Extracellular ATP^{4-} promotes cation fluxes in the J774 mouse macrophage cell line. J Biol Chem 1987;262:3118–22.
[14] Greenberg S, Di Virgilio F, Steinberg TH, Silverstein SC. Extracellular nucleotides mediate Ca^{2+} fluxes in J774 macrophages by two distinct mechanisms. J Biol Chem 1988;263:10337–43.
[15] Chen BC, Lin WW. Pyrimidinoceptor potentiation of macrophage PGE(2) release involved in the induction of nitric oxide synthase. Br J Pharmacol 2000;30:777–86.
[16] Di Virgilio F, Chiozzi P, Ferrari D, Falzoni S, Sanz JM, Morelli A, et al. Nucleotide receptors: an emerging family of regulatory molecules in blood cells. Blood 2001;97:587–600.
[17] Deuchars SA, Atkinson L, Brooke RE, Musa H, Milligan CJ, Batten TF, et al. Neuronal $P2X_7$ receptors are targeted to presynaptic terminals in the central and peripheral nervous systems. J Neurosci 2001;21:7143–52.
[18] Glass R, Burnstock G. Immunohistochemical identification of cells expressing ATP-gated cation channels (P2X receptors) in the adult rat thyroid. J Anat 2001;198:569–79.
[19] Hoebertz A, Townsend-Nicholson A, Glass R, Burnstock G, Arnett TR. Expression of P2 receptors in bone and cultured bone cells. Bone 2000;27:503–10.
[20] Lee H-Y, Bardini M, Burnstock G. Distribution of P2X receptors in the urinary bladder and ureter of the rat. J Urol 2000;163:2002–7.
[21] Panenka W, Jijon H, Herx LM, Armstrong JN, Feighan D, Wei T, et al. $P2X_7$-like receptor activation in astrocytes increases chemokine monocyte chemoattractant protein-1 expression via mitogen-activated protein kinase. J Neurosci 2001;21:7135–42.
[22] Sluyter R, Barden JA, Wiley JS. Detection of P2X purinergic receptors on human B lymphocytes. Cell Tissue Res 2001;304:231–6.
[23] Glass R, Townsend-Nicholson A, Burnstock G. P2 receptors in the thymus: expression of P2X and P2Y receptors in adult rats, an immunohistochemical and in situ hybridisation study. Cell Tissue Res 2000;300:295–306.
[24] Berchtold S, Ogilvie AL, Bogdan C, Muhl-Zurbes P, Ogilvie A, Schuler G, et al. Human monocyte derived dendritic cells express functional P2X and P2Y receptors as well as ecto-nucleotidases. FEBS Lett 1999;458:424–8.
[25] Ferrari D, La Sala A, Chiozzi P, Morelli A, Falzoni S, Girolomoni G, et al. The P2 purinergic receptors of human dendritic cells: identification and coupling to cytokine release. FASEB J 2000;14:2466–76.
[26] Bowler JW, Bailey RJ, North RA, Surprenant A. P2X4, P2Y1 and P2Y2 receptors on rat alveolar macrophages. Br J Pharmacol 2003;140:567–75.
[27] Bradford MM. A rapid and sensitive method for the quantitation of microgram quantities of protein utilizing the principle of protein-dye binding. Anal Biochem 1976;72:248–54.
[28] Llewellyn-Smith IJ, Pilowsky P, Minson JB. The tungstate-stabilized tetramethylbenzidine reaction for light and electron microscopic immunocytochemistry and for revealing biocytin-filled neurons. J Neurosci Methods 1993;46:27–40.
[29] Oglesby IB, Lachnit WG, Burnstock G, Ford APDW. Subunit specificity of polyclonal antisera to the carboxy terminal regions

of P2X receptors $P2X_1$ through $P2X_7$. Drug Dev Res 1999;47: 189–95.
[30] Bailey MA, Imbert-Teboul M, Turner C, Marsy S, Srai K, Burnstock G, et al. Axial distribution and characterization of basolateral P2Y receptors along the rat renal tubule. Kidney Int 2000;58:1893–901.
[31] Bailey MA, Imbert-Teboul M, Turner C, Srai SK, Burnstock G, Unwin RJ. Evidence for basolateral $P2Y_6$ receptors along the rat proximal tubule: functional and molecular characterization. J Am Soc Nephrol 2001;12:1640–7.
[32] Fredholm BB, Abbracchio MP, Burnstock G, Daly JW, Harden TK, Jacobson KA, et al. Nomenclature and classification of purinoceptors. Pharmacol Rev 1994;46:143–56.
[33] Bisaggio RC, Nihei OK, Persechini PM, Savino W, Alves LA. Characterization of P2 receptors in thymic epithelial cells. Cell Mol Biol 2001;47:19–31.
[34] Kuznetsov V, Pak E, Robinson RB, Steinberg SF. β2-adrenergic receptor actions in neonatal and adult rat ventricular myocytes. Circ Res 1995;76:40–52.
[35] Dunn PM, Benton DC, Campos RJ, Ganellin CR, Jenkinson DH. Discrimination between subtypes of apamin-sensitive Ca^{2+}-activated K^+ channels by gallamine and a novel bis-quaternary quinolinium cyclophane, UCL 1530. Br J Pharmacol 1996;117:35–42.
[36] Hamill OP, Marty A, Neher E, Sakmann B, Sigworth FJ. Improved patch-clamp techniques for high-resolution current recording from cells and cell-free membrane patches. Pflugers Arch 1981;391:85–100.
[37] Horn R, Marty A. Muscarinic activation of ionic currents measured by a new whole-cell recording method. J Gen Physiol 1988;92:145–59.
[38] Albuquerque C, Oliveira SM, Coutinho-Silva R, Oliveira-Castro GM, Persechini PM. ATP- and UTP-induced currents in macrophages and macrophage polykaryons. Am J Physiol 1993;265:C1663–73.
[39] Burnstock G. Overview of P2 receptors: possible functions in immune cells. Drug Dev Res 2001;53:53–9.
[40] Ferrari D, Idzko M, Dichmann S, Purlis D, Virchow C, Norgauer J, et al. P2 purinergic receptors of human eosinophils: characterization and coupling to oxygen radical production. FEBS Lett 2000;486: 217–24.
[41] Alves LA, Coutinho-Silva R, Savino W, Extracellular. ATP: a further modulator in neuroendocrine control of the thymus. Neuroimmunomodulation 1999;6:81–9.
[42] Chvatchko Y, Valera S, Aubry JP, Renno T, Buell G, Bonnefoy JY. The involvement of an ATP-gated ion channel, $P2X_1$, in thymocyte apoptosis. Immunity 1996;5:275–83.
[43] Adrian K, Bernhard MK, Breitinger H-G, Ogilvie A. Expression of purinergic receptors (ionotropic $P2X_{1-7}$ and metabotropic $P2Y_{1-11}$) during myeloid differentiation of HL60 cells. Biochim Biophys Acta 2000;1492:127–38.
[44] Buell G, Michel AD, Lewis C, Collo G, Humphrey PP, Surprenant A. $P2X_1$ receptor activation in HL60 cells. Blood 1996;87:2659–64.
[45] Clifford EE, Parker K, Humphreys BD, Kertesy SB, Dubyak GR. The $P2X_1$ receptor, an adenosine triphosphate-gated cation channel, is expressed in human platelets but not in human blood leukocytes. Blood 1998;91:3172–81.
[46] Burnstock G. P2X receptors in sensory neurones. Br J Anaesth 2000;84:476–88.
[47] Burnstock G. Purine-mediated signalling in pain and visceral perception. Trends Pharmacol Sci 2001;22:182–818.
[48] Bobanovic LK, Royle SJ, Murrell-Lagnado RD. P2X receptor trafficking in neurons is subunit specific. J Neurosci 2002;22:4814–24.
[49] Eschke D, Wust M, Hauschildt S, Nieber K. Pharmacological characterization of the P2X(7) receptor on human macrophages using the patch-clamp technique. Naunyn Schmiedebergs Arch Pharmacol 2002;365:168–71.
[50] Jones CA, Vial C, Sellers LA, Humphrey PP, Evans RJ, Chessell IP. Functional regulation of $P2X_6$ receptors by N-linked glycosylation: identification of a novel alpha beta-methylene ATP-sensitive phenotype. Mol Pharmacol 2004;65:979–85.
[51] Torres GE, Egan TM, Voigt MM. Hetero-oligomeric assembly of P2X receptor subunits. Specificities exist with regard to possible partners. J Biol Chem 1999;274:6653–9.